Universal correlations in driven binary mixtures

Alexis Poncet,[1,2] Olivier Bénichou,[3] Vincent Démery,[1] and Gleb Oshanin[3]

[1] *Gulliver, CNRS, ESPCI Paris, PSL Research University, 10 rue Vauquelin, Paris, France*
[2] *Département de Physique, ENS, 24 Rue Lhomond, 75005 Paris, France*
[3] *Laboratoire de Physique Théorique de la Matière Condensée, CNRS/UPMC, 4 Place Jussieu, F-75005 Paris, France*

Several tracers pulled in a quiescent colloidal suspension can spontaneously cooperate in order to increase their mobility. Here, we characterize the cooperativity in a driven binary mixture, where we analytically compute the correlations by linearizing the stochastic equations for the density fields, which is valid for a dense suspension of soft particles. The correlations are found to be long ranged, with a universal algebraic decay and transverse profile. Brownian dynamics simulations confirm our results and show that the universal shape holds far from the validity range of our computation.

A lonely tracer moving through a dense environment sees its motion hindered by the surrounding bath particles [1, 2]. When several tracers are biased in the same direction, they may act cooperatively in order to reduce their drag [3], like pedestrians walking in a crowd [4] (see Fig. 1). They may even seggregate and form lanes, thereby recovering their mobility in the absence of bath particles [5, 6]. Despite a lot of efforts, some fundamental questions remain open: what are the correlations between the tracers, and is it possible to define a correlation length? Does the formation of lanes correspond to a non-equilibrium phase transition, where this correlation length diverges?

The correlation between the tracers and the bath particles is reminiscent of the wake created by a *single* tracer, which is relevant for microrheology [1, 7, 8]. It has been computed in different models: Brownian dilute hard spheres [9], dense soft spheres [10] or hard core particles on a lattice [11]. In the two last cases, the density was found to relax algebraically behind the tracer, with an exponent $(d+1)/2$, where d is the dimension of space.

On the other hand, the situation where *half* of the particles of a binary mixture are submitted to an external force and the other half to the opposite force can be realized with ions or charged colloids submitted to an electrical field [6]. At large enough forces, the particles form lanes parallel to the field, but the nature of this "laning transition" remains unclear [5, 12–17]. Recently, the correlations have been measured in simulations of a 2-dimensional system and predicted using a numerical integration of a closure of the N-particles Fokker-Planck equation [14]. An algebraic decay in the direction of the field has been conjectured from the simulations, with an exponent comprised between 1 and 2, and it has been argued that it could be related to a diverging correlation length, and thus to a phase transition. In order to confirm this conjecture, it is crucial to analytically determine the shape and long-distance behavior of the correlations.

Here, we analytically compute the correlations using a linearized Stochastic Density Functional Theory (LSDFT), which was introduced recently to compute the correlations in an electrolyte [18] and is valid for a dense system of soft particles. We show that they decay algebraically with an exponent $(d+1)/2$ at any value of the external force, in both directions along the field. Moreover, we find that they have a universal shape in the transverse direction. This behavior rests on simple assumptions, suggesting that it is universal. Brownian dynamics simulations of harmonic spheres agree quantitatively with our predictions, and confirm that the scaling and the shape of the correlations hold far beyond the validity regime of LSDFT.

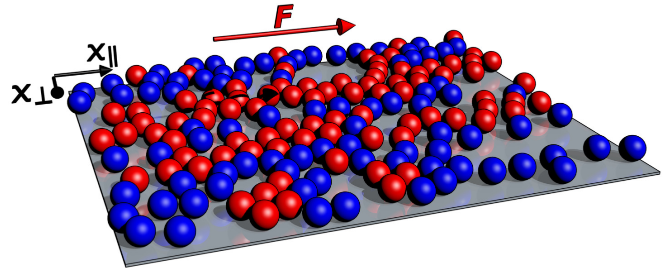

FIG. 1. Brownian interacting particles in two dimensions. The "tracers" (red) are submitted to an external force $\boldsymbol{F}$ while the "non tracers" (blue) are not. Particles of the same species tend to form lanes in the direction of the field and reduce their drag. Snapshot of numerical simulations of harmonic spheres with $\bar{\rho} = 0.5$, $\tau = 0.5$, $T = 10^{-4}$ and $F = 0.005$.

Model – We use a continuous description where N particles, located at $\boldsymbol{x}_i(t) \in \mathbb{R}^d$, interact via an isotropic pair potential $V(x)$ [5, 14, 15]. The $\tau_1 N = \tau N$ "tracers", $i \in \mathcal{T}_1 = \mathcal{T}$, are submitted to an external force $\boldsymbol{F}$, while the $\tau_2 N = (1-\tau)N$ "non tracers", $i \in \mathcal{T}_2 = \bar{\mathcal{T}}$, are not (Fig. 1). We assume an overdamped Langevin dynamics:

$$\dot{\boldsymbol{x}}_i(t) = \mathbb{1}_{i\in\mathcal{T}}\boldsymbol{F} - \sum_{j\neq i} \nabla V(\boldsymbol{x}_i(t) - \boldsymbol{x}_j(t)) + \boldsymbol{\eta}_i(t), \quad (1)$$

where the Gaussian white noise $\boldsymbol{\eta}_i(t)$ has a correlation function $\langle \boldsymbol{\eta}_i(t)\boldsymbol{\eta}_j(t')^{\mathrm{T}}\rangle = 2T\delta_{ij}\delta(t-t')\mathbb{1}$, where T is the temperature. Considering that the non tracers are not submitted to any force is not a restriction, since by symmetry arguments only the difference of the forces applied to the two species affect the correlations [5].

In order to quantify the cooperativity, we introduce the effective mobility $\kappa_{\rm eff}$ of the tracers as $\langle \dot{\boldsymbol{x}}_i \rangle = \kappa_{\rm eff}\boldsymbol{F}$ for $i \in \mathcal{T}$. In the absence of interactions, the bare mobility is $\kappa_0 = 1$. Using symmetry arguments (see SM I), one can show that

$$\kappa_{\rm eff}(\tau) = 1 - (1-\tau)K(\tau), \tag{2}$$

where $K(\tau) = K(1-\tau)$. The factor $1-\tau$ comes from the density of bath particles which hinders the motion of the tracers, and $K(\tau)$ describes the cooperativity of the tracers.

We define the microscopic densities

$$\rho_\alpha(\boldsymbol{x},t) = \sum_{i\in\mathcal{T}_\alpha} \delta(\boldsymbol{x} - \boldsymbol{x}_i(t)); \tag{3}$$

their spatial average is $\bar{\rho}_\alpha = \tau_\alpha \bar{\rho}$, where $\bar{\rho} = N/\mathcal{V}$, $\mathcal{V}$ being the volume of the system. We introduce the pair correlation functions as [19]

$$h_{\alpha\beta}(\boldsymbol{x}) = \left\langle \left[\frac{\rho_\alpha(\boldsymbol{x})}{\bar{\rho}_\alpha} - 1\right]\left[\frac{\rho_\beta(0)}{\bar{\rho}_\beta} - 1\right]\right\rangle. \tag{4}$$

Averaging Eq. (1) and using the pair correlation functions, K can be expressed as (see SM II)

$$K = \frac{\bar{\rho}}{F}\int \partial_\parallel V(\boldsymbol{x}) h_{12}(\boldsymbol{x})\mathrm{d}\boldsymbol{x}; \tag{5}$$

the index $\parallel$ denotes the direction parallel to the external force

Mean-field calculation – In order to compute the correlation functions, we use the Dean-Kawasaki equation for the density fields (or Stochastic Density Functional Theory, SDFT) [18, 20, 21]:

$$\dot{\rho}_\alpha = \nabla\cdot\left[T\nabla\rho_\alpha - \delta_{\alpha 1}\rho_\alpha \boldsymbol{F} + \rho_\alpha \sum_\beta \nabla V * \rho_\beta + \rho_\alpha^{1/2}\boldsymbol{\eta}_\alpha\right], \tag{6}$$

where $\boldsymbol{\eta}_\alpha(\boldsymbol{x},t)$ is a Gaussian noise with correlations $\langle \boldsymbol{\eta}_\alpha(\boldsymbol{x},t)\boldsymbol{\eta}_\beta(\boldsymbol{x}',t')^{\rm T}\rangle = 2T\delta_{\alpha\beta}\delta(\boldsymbol{x}-\boldsymbol{x}')\delta(t-t')\mathbb{1}$. This equation is exact, but it is non-linear and contains multiplicative noise, it is thus difficult to handle. However, it can be linearized by assuming small density fluctuations: $\rho_\alpha(\boldsymbol{x},t) - \bar{\rho}_\alpha = \rho_\alpha^{1/2}\phi_\alpha(\boldsymbol{x},t) \ll \bar{\rho}_\alpha$ [10]. Under this assumption, it reads in Fourier space (with convention $\tilde{h}(\boldsymbol{k}) = \int h(\boldsymbol{x})\mathrm{e}^{-\mathrm{i}\boldsymbol{k}\cdot\boldsymbol{x}}\mathrm{d}\boldsymbol{x}$)

$$\partial_t \tilde{\phi}_\alpha = -k^2 \sum_\beta \tilde{A}_{\alpha\beta}\tilde{\phi}_\beta + \tilde{\xi}_\alpha, \tag{7}$$

where

$$\tilde{A}(\boldsymbol{k}) = T\begin{pmatrix} 1 + \mathrm{i}\frac{fk_\parallel}{k^2} + \tau_1\tilde{v}(\boldsymbol{k}) & \sqrt{\tau_1\tau_2}\tilde{v}(\boldsymbol{k}) \\ \sqrt{\tau_1\tau_2}\tilde{v}(\boldsymbol{k}) & 1 + \tau_2\tilde{v}(\boldsymbol{k}) \end{pmatrix} \tag{8}$$

and the Gaussian noise $\tilde{\xi}(\boldsymbol{k},t)$ has correlations $\langle \tilde{\xi}_\alpha(\boldsymbol{k},t)\tilde{\xi}_\beta(\boldsymbol{k}',t')\rangle = 2(2\pi)^d T\delta_{\alpha\beta}\delta(\boldsymbol{k}+\boldsymbol{k}')\delta(t-t')k^2$. We have introduced the Péclet number $f = F/T$ and the rescaled potential $v = \bar{\rho}V/T$. The linearization of Eq. (6) is valid in the large density limit, $\bar{\rho}\to\infty$, with v kept constant, meaning that the suspension is very dense and soft [10].

The correlation functions of the fields ϕ, $C_{\alpha\beta}(\boldsymbol{x}) = \langle \phi_\alpha(\boldsymbol{x},t)\phi_\beta(0,t)\rangle$ are related to the pair correlation functions (4) by $h_{\alpha\beta} = C_{\alpha\beta}/\sqrt{\bar{\rho}_\alpha\bar{\rho}_\beta}$. In the stationnary regime, they satisfy [22]

$$\tilde{A}\tilde{C} + \tilde{C}\tilde{A}^* = 2T\mathbb{1}. \tag{9}$$

At equilibrium, *i.e.*, without external force, $\tilde{A}^* = \tilde{A}$ and the equilibrium correlation functions $\tilde{C} = T\tilde{A}^{-1}$ are recovered. In the general case, the solution reads (see SM III):

$$\tilde{C} = \left[(1+\tilde{v})(2+\tilde{v})^2 + (1+\tilde{v}+\tau_1\tau_2\tilde{v}^2)\frac{f^2k_\parallel^2}{k^4}\right]^{-1} \begin{pmatrix} (1+\tau_2\tilde{v})\left[(2+\tilde{v})^2 + \frac{f^2k_\parallel^2}{k^4}\right] & -\sqrt{\tau_1\tau_2}\tilde{v}(2+\tilde{v})(2+\tilde{v}-\mathrm{i}\frac{fk_\parallel}{k^2}) \\ -\sqrt{\tau_1\tau_2}\tilde{v}(2+\tilde{v})(2+\tilde{v}+\mathrm{i}\frac{fk_\parallel}{k^2}) & (1+\tau_1\tilde{v})\left[(2+\tilde{v})^2 + \frac{f^2k_\parallel^2}{k^4}\right] \end{pmatrix} \tag{10}$$

This expression allows to determine the function K entering the mobility:

$$K = \frac{1}{\bar{\rho}}\times \int \frac{\tilde{v}^2(2+\tilde{v})k_\parallel^2 k^2}{(1+\tilde{v})(2+\tilde{v})^2k^4 + [1+\tilde{v}+\tau(1-\tau)\tilde{v}^2]f^2k_\parallel^2}\frac{\mathrm{d}\boldsymbol{k}}{(2\pi)^d}. \tag{11}$$

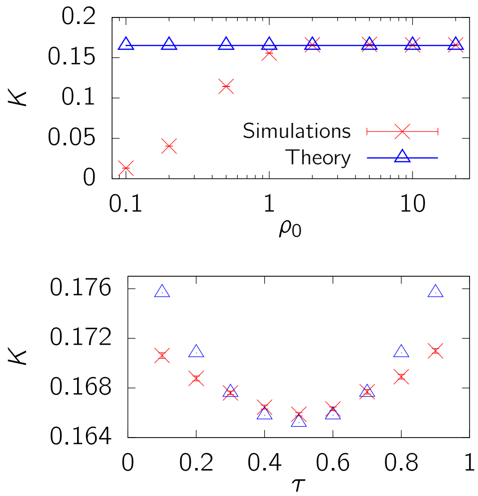

FIG. 2. Cooperativity of the tracers K in $d = 2$. *Top:* K as a function of $\bar{\rho}$ with $\bar{\rho}/T = 10$, $F/T = 20$ and $\tau = 0.5$, analytical prediction (solid line) and simulations (points). *Bottom:* K as a function of the fraction of tracers τ for $\bar{\rho} = 2$, $\bar{\rho}/T = 10$ and $F/T = 20$, analytical prediction (solid line) and simulations (points).

In the limit $\tau = 0$, the mobility found for a single tracer is recovered [10] (Eq. (79)). K is minimal (*i.e.*, the cooperativity is maximal) for $\tau = 1/2$ (Fig. 2).

Long distance behavior – The correlation functions Eq. (43) are not continuous at 0 (the limits $k_\parallel \to 0$ and $k_\perp \to 0$ do not commute); this points to an algebraic decay. In order to determine the long distance behavior, we introduce

$$\tilde{C}_a(k_\parallel, \boldsymbol{k}_\perp) = \tilde{C}(ak_\parallel, a^\zeta \boldsymbol{k}_\perp), \tag{12}$$

where ζ is an exponent characterizing the relative scaling of the longitudinal and transverse directions, and take the limit $a \to 0$. The terms $fk_\parallel/k^2$ set $\zeta = 1/2$; then the limit $a \to 0$ amounts to replace $\tilde{v}(\boldsymbol{k}) \to \tilde{v}(0) = v_0$ and $fk_\parallel/k^2 \to fk_\parallel/k_\perp^2$ in Eq. (43). Now, the inverse Fourier transform can be obtained analytically (see SM IV), leading to

$$h_{\alpha\beta}(\boldsymbol{x}) \approx_{x_\parallel \to \pm\infty} \frac{H^\pm_{\alpha\beta}}{|x_\parallel|^{\frac{d+1}{2}}} g\left(\frac{\boldsymbol{x}_\perp}{\sqrt{D|x_\parallel|}}\right), \tag{13}$$

where

$$g(\boldsymbol{u}) = \nabla^2_{\boldsymbol{u}}\left(\mathrm{e}^{-\boldsymbol{u}^2/2}\right), \tag{14}$$

$$D = \frac{2(2+v_0)}{\beta f}, \tag{15}$$

$$H^\pm_{11} = -\frac{(1-\tau)v_0^2[1+(1-\tau)v_0]\beta^{\frac{d-5}{2}} f^{\frac{d-1}{2}}}{2^{d+1}\pi^{\frac{d-1}{2}}\bar{\rho}(1+v_0)^2(2+v_0)^{\frac{d-1}{2}}}, \tag{16}$$

$$H^\pm_{21} = \frac{v_0\beta^{\frac{d-1}{2}}(1\mp\beta^{-1})f^{\frac{d-1}{2}}}{2^{d+1}\pi^{\frac{d-1}{2}}\bar{\rho}(1+v_0)(2+v_0)^{\frac{d-1}{2}}}. \tag{17}$$

We defined $\beta = \left[1 + \tau(1-\tau)\frac{v_0^2}{1+v_0}\right]^{1/2}$.

Eqs. (13–17) are our main results. First, they allow to recover the algebraic decay with power $(d+1)/2$ of the depletion wake behind a single tracer [10]; they also extend this result by giving the shape of the wake. At vanishing tracers density ($\tau \to 0$), $\beta \to 1$ and so $H^+_{21} \to 0$, and the decay of h_{21} in front of the tracers is exponential (see SM V). Second, for a finite density of tracers, they show that the algebraic decay and shape holds also for the tracer-non tracer correlation h_{21} in front of the tracers ($x_\parallel \to \infty$), and for the tracer-tracer correlation h_{11}. The tracer-tracer correlation is positive along the axis $\boldsymbol{x}_\perp = 0$, indicating a tendency to form lanes.

Numerical simulations – We have performed two dimensional Brownian dynamics simulations of Eq. (1) with $N = 10^4$ particles for harmonic spheres, corresponding to the pair potential $V(\boldsymbol{x}) = (1-|\boldsymbol{x}|)^2\theta(1-|\boldsymbol{x}|)/2$, where $\theta(u)$ is the Heaviside function. We used a square box with periodic boundary conditions.

The mobility is shown as a function of $\bar{\rho}$ with $\bar{\rho}/T$ and f kept constant in Fig. 2 (*Top*). The result from the simulations converges to the analytical prediction as $\bar{\rho} \to \infty$, which is the condition of validity of our computation. Varying the fraction of tracers τ, the mobility displays a minimum at $\tau = 0.5$, which is correctly predicted by the theory (Fig. 2, *Bottom*).

The correlation functions for $\bar{\rho} = 2$, $T = 0.2$ and $f = 20$ are shown on Fig. 3, and are compared to the numerical integration of Eq. (43). Cuts along the transverse direction, rescaled using Eq. (13), are compared to the numerical integration on Fig. 4 and to the shape (14). A good collapse is found, which confirms the scaling laws, and a quantitative agreement is found for the shape.

Universality – For a single tracer, the same algebraic decay was found both for hard core particles on a lattice [11] and for soft Brownian particles [10], suggesting a universal behavior. We now argue that the scaling (13) of the correlations and their shape (14), hold far from the validity regime of our computation, namely a dense and soft suspension.

Eq. (13) has a simple interpretation as a diffusive process. Replacing $x_\parallel$ (or $-x_\parallel$, depending on the direction of interest) by the time and $\boldsymbol{x}_\perp$ by the position, Eq. (13) is the solution of a diffusion equation where the source is the second derivative of a Dirac distribution (notably, it is symmetric and its integral is zero). This behavior emanates from simple properties of our system: (i) The long-distance dynamics without external force is diffusive (*i.e.*, the relaxation rate of $\tilde{\phi}(\boldsymbol{k})$ scales as k^2 for small k); (ii) The tracers have a finite average velocity; (iii) The number of particles is conserved. This suggests that the correlations have the same behavior in any system sharing these properties. Notably, this is the case of a dilute bath of Brownian hard spheres, and the equations for the wake behind a single tracer in this system are compatible with Eqs. (13,14) [9] (Eqs. (16-17)).

To test this hypothesis, we simulated our system of

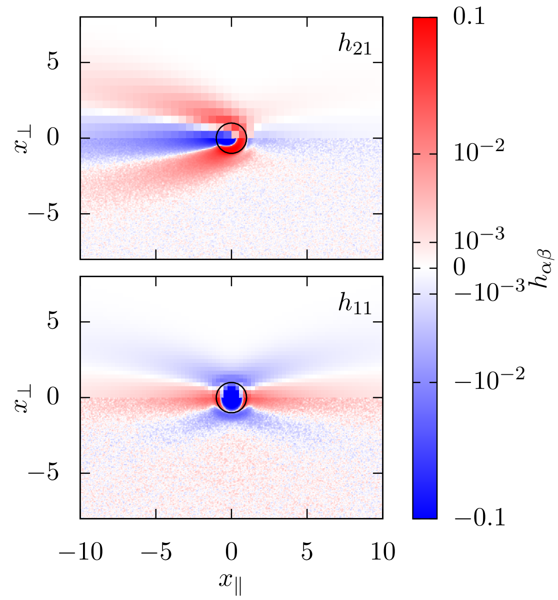

FIG. 3. Pair correlations functions from the simulations (lower half) and the theory (upper half) for $\bar{\rho}=2$, $T=0.2$, $F=4$ and $\tau=0.5$, in dimension $d=2$. The black circle has the size of a particle. *Top:* tracer-non tracers correlation. *Bottom:* tracer-tracer correlation.

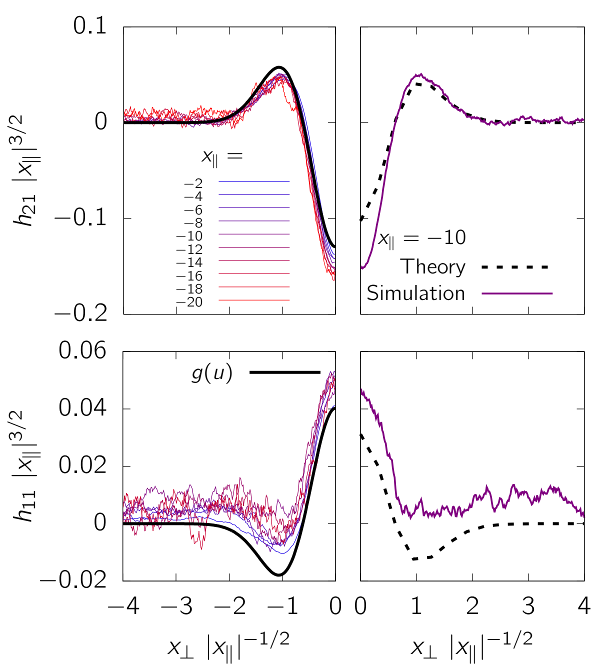

FIG. 4. Rescaled tranverse profiles of the pair correlation functions for $\bar{\rho}=2$, $T=0.2$, $F=4$, $\tau=0.5$, in dimension $d=2$. *Left panel:* transverse profiles from the simulations at different longitudinal positions and universal shape Eq. (14) (thick black line). *Right panel:* transverse profile at $x_\parallel = -10$ from the simulations (solid line) and analytical prediction obtained by numerical inversion of Eq. (43) (dashed line). *Top:* tracer-non tracers correlation. *Bottom:* tracer-tracer correlation.

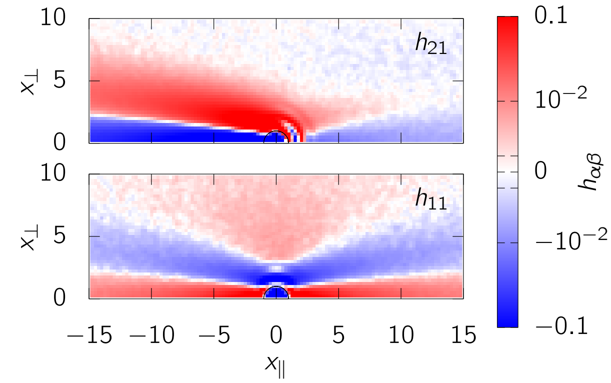

FIG. 5. Pair correlations functions from the simulations for $\bar{\rho}=0.2$, $T=0.001$, $F=0.02$, $\tau=0.5$, in dimension $d=2$. The black circle has the size of a particle. *Top:* tracer-non tracers correlation. *Bottom:* tracer-tracer correlation.

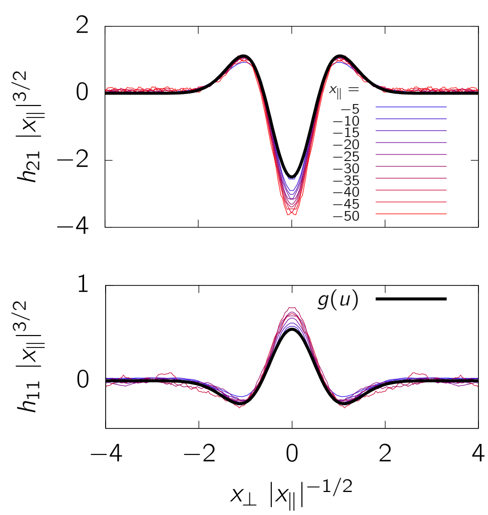

FIG. 6. Rescaled tranverse profiles of the pair correlation functions for $\bar{\rho}=0.2$, $T=0.001$, $F=0.02$, $\tau=0.5$, in dimension $d=2$. The transverse profiles from the simulations at different longitudinal positions are shown together with the universal shape Eq. (14) with fitted height and width (thick black line). *Top:* tracer-non tracers correlation. *Bottom:* tracer-tracer correlation.

harmonic spheres in the dilute and hard regime: $\bar{\rho}=0.2$, $T=10^{-3}$, $f=20$. The correlations are shown in Fig. 5 and they have the same shape as in the opposite limit of dense and soft particles. Rescaled transverse cuts are shown on Fig. 6: a very good collapse is found, and the shape is well described by Eq. (14) with fitted height and width.

Laning – Our results partly confirm the conjecture of Ref. [14]: the correlation functions are long-ranged below the laning transition (if it exists) and the exponent, 3/2 in $d=2$ is compatible with the value reported in Ref. [14]. However, our conclusion is different: this algebraic decay is not associated to a divergence in the structure factors, but only to a discontinuity.

The algebraic decay implies that the correlation length defined in Ref. [15] does not correspond to an exponential decay of the correlations.

Finally, we note that the algebraic decay of the correlations cannot hold if the particles are completely seggregated into oppositely-moving lanes, where the correlations should converge to a finite value as $x_\parallel \to \infty$. However, Ref. [15] suggests that the seggregation is never complete, hence the universal form of the correlations may hold at any value of the applied force.

Conclusion – Using linearized SDFT, we have computed the correlations and mobility in a driven binary mixture in the limit of large density and weak interactions. The correlations decay algebraically in the direction of the external force, with a self-similar profile. We showed that this behavior holds far from the validity regime of our computations.

An interesting extension of the present work would consider an inertial system [23], which can be used to model a plasma [24]. The linearized SDFT recently proposed for such system suggests that the correlations may have a different scaling at long distances [25].

[1] A. Meyer, A. Marshall, B. G. Bush, and E. M. Furst, Journal of Rheology **50**, 77 (2006).

[2] R. Candelier and O. Dauchot, Phys. Rev. E **81**, 011304 (2010).

[3] C. Mejia-Monasterio and G. Oshanin, Soft Matter **7**, 993 (2011).

[4] M. Moussaïd, E. G. Guillot, M. Moreau, J. Fehrenbach, O. Chabiron, S. Lemercier, J. Pettré, C. Appert-Rolland, P. Degond, and G. Theraulaz, PLoS Comput Biol **8**, 1 (2012).

[5] J. Dzubiella, G. P. Hoffmann, and H. Löwen, Phys. Rev. E **65**, 021402 (2002).

[6] T. Vissers, A. Wysocki, M. Rex, H. Lowen, C. P. Royall, A. Imhof, and A. van Blaaderen, Soft Matter **7**, 2352 (2011).

[7] L. G. Wilson and W. C. K. Poon, Phys. Chem. Chem. Phys. **13**, 10617 (2011).

[8] E. Nazockdast and J. F. Morris, Journal of Rheology **60**, 733 (2016).

[9] T. M. Squires and J. F. Brady, Physics of Fluids (1994-present) **17**, 073101 (2005).

[10] V. Démery, O. Bénichou, and H. Jacquin, New Journal of Physics **16**, 053032 (2014).

[11] O. Bénichou, A. M. Cazabat, J. De Coninck, M. Moreau, and G. Oshanin, Phys. Rev. Lett. **84**, 511 (2000).

[12] J. Chakrabarti, J. Dzubiella, and H. Löwen, EPL (Europhysics Letters) **61**, 415 (2003).

[13] J. Chakrabarti, J. Dzubiella, and H. Löwen, Phys. Rev. E **70**, 012401 (2004).

[14] M. Kohl, A. V. Ivlev, P. Brandt, G. E. Morfill, and H. Löwen, Journal of Physics: Condensed Matter **24**, 464115 (2012).

[15] T. Glanz and H. Löwen, Journal of Physics: Condensed Matter **24**, 464114 (2012).

[16] E. M. Foulaadvand and B. Aghaee, The European Physical Journal E **39**, 1 (2016).

[17] K. Klymko, P. L. Geissler, and S. Whitelam, ArXiv e-prints (2016), arXiv:1602.01878 [cond-mat.stat-mech].

[18] V. Démery and D. S. Dean, Journal of Statistical Mechanics: Theory and Experiment **2016**, 023106 (2016).

[19] J.-P. Hansen and I. R. McDonald, *Theory of Simple Liquids*, 3rd ed. (London: Academic Press, 2006).

[20] K. Kawasaki, Physica A: Statistical Mechanics and its Applications **208**, 35 (1994).

[21] D. S. Dean, Journal of Physics A: Mathematical and General **29**, L613 (1996).

[22] R. Zwanzig, *Nonequilibrium statistical mechanics* (Oxford University Press, USA, 2001).

[23] X. Liu, W. Ge, and J. Li, Powder Technology **184**, 224 (2008).

[24] K. R. Sütterlin, A. Wysocki, A. V. Ivlev, C. Räth, H. M. Thomas, M. Rubin-Zuzic, W. J. Goedheer, V. E. Fortov, A. M. Lipaev, V. I. Molotkov, O. F. Petrov, G. E. Morfill, and H. Löwen, Phys. Rev. Lett. **102**, 085003 (2009).

[25] V. Démery, Phys. Rev. E **91**, 062301 (2015).

Universal correlations in driven binary mixtures Supplemental Material

I. SYMMETRY ARGUMENTS FOR THE EFFECTIVE MOBILITY

Here we link the effective mobility at a tracer fraction $1-\tau$ to the one at a fraction τ. Let $F_{/1}$ (resp. $F_{/2}$) the force applied to one tracer (resp. one non-tracer) by all the other particles, the effective mobility is

$$\kappa_{\text{eff}}(\tau) = \frac{\langle \dot{x}_{1\parallel} \rangle}{F} = \frac{F + \langle F_{/1} \rangle}{F} = 1 + \frac{\langle F_{/1} \rangle}{F}. \tag{18}$$

Let us now add a force $-F$ on all the particles. This leads to consider the particles 2 as the tracers. But the addition of an external force only translates the system at a constant velocity $-F$, hence the correlation functions are not modified, and neither do the internal forces ($F_{/1}$ and $F_{/2}$). The effective mobility as tracer fraction $1-\tau$ is given by

$$\kappa_{\text{eff}}(1-\tau) = \frac{\langle \dot{x}_{2\parallel} \rangle}{-F} = \frac{-F + \langle F_{/2} \rangle}{-F} = 1 - \frac{\langle F_{/2} \rangle}{F}. \tag{19}$$

Introducing $\Delta\kappa = 1 - \kappa_{\text{eff}}$, we get

$$\frac{\Delta\kappa(\tau)}{\Delta\kappa(1-\tau)} = -\frac{\langle F_{/1} \rangle}{\langle F_{/2} \rangle}. \tag{20}$$

The third law of Newton for the inter-particle interactions gives:

$$\tau \langle F_{/1} \rangle + (1-\tau) \langle F_{/2} \rangle = 0, \tag{21}$$

leading to

$$\frac{\Delta\kappa(\tau)}{\Delta\kappa(1-\tau)} = \frac{1-\tau}{\tau}. \tag{22}$$

Introducing $K(\tau) = \Delta\kappa(\tau)/(1-\tau)$ allows to rewrite it as

$$\kappa_{\text{eff}}(\tau) = 1 - (1-\tau)K(\tau), \tag{23}$$

$$K(\tau) = K(1-\tau). \tag{24}$$

II. EFFECTIVE MOBILITY FROM THE CORRELATION FUNCTIONS

In this section, we prove Eq. (5). Averaging Eq. (1) and summing over the tracers, we get

$$\sum_{i\in\mathcal{T}} \langle \dot{\boldsymbol{x}}_i \rangle = \tau N \boldsymbol{F} - \sum_{i\in\mathcal{T}} \sum_{j\neq i} \langle \nabla V(\boldsymbol{x}_i - \boldsymbol{x}_j) \rangle. \tag{25}$$

The left-hand side is $\tau N \kappa_{\text{eff}} \boldsymbol{F}$, hence a projection onto the direction parallel to the force leads to

$$\kappa_{\text{eff}} = 1 - \frac{1}{\tau N F} \left\langle \sum_{i\in\mathcal{T}} \sum_{j\neq i} \partial_\parallel V(\boldsymbol{x}_i - \boldsymbol{x}_j) \right\rangle. \tag{26}$$

Since the potential is isotropic, $\nabla V(0) = 0$; this allows us to include all the particles in the second sum in the previous equation. The sums can then be rewritten using the density fields $\rho_\alpha(\boldsymbol{x})$:

$$\sum_{i\in\mathcal{T}} \sum_{j} \partial_\parallel V(\boldsymbol{x}_i - \boldsymbol{x}_j) = \int \rho_1(\boldsymbol{x})[\rho_1(\boldsymbol{x}') + \rho_2(\boldsymbol{x}')] \partial_\parallel V(\boldsymbol{x} - \boldsymbol{x}') \mathrm{d}\boldsymbol{x} \mathrm{d}\boldsymbol{x}'. \tag{27}$$

The average can be expressed with the pair correlation functions defined in Eq. (4), $\langle \rho_\alpha(\boldsymbol{x})\rho_\beta(\boldsymbol{x}')\rangle = \bar{\rho}_\alpha\bar{\rho}_\beta[1 + h_{\alpha\beta}(\boldsymbol{x}-\boldsymbol{x}')]$. This leads to

$$\left\langle \sum_{i\in\mathcal{T}}\sum_j \partial_\parallel V(\boldsymbol{x}_i-\boldsymbol{x}_j)\right\rangle = \mathcal{V}\bar{\rho}_1^2\int[1+h_{11}(\boldsymbol{x})]\partial_\parallel V(\boldsymbol{x})\mathrm{d}\boldsymbol{x} + \mathcal{V}\bar{\rho}_1\bar{\rho}_2\int[1+h_{12}(\boldsymbol{x})]\partial_\parallel V(\boldsymbol{x})\mathrm{d}\boldsymbol{x} \tag{28}$$

$$= \mathcal{V}\bar{\rho}_1\bar{\rho}_2\int h_{12}(\boldsymbol{x})\partial_\parallel V(\boldsymbol{x})\mathrm{d}\boldsymbol{x}. \tag{29}$$

The last equation is obtained from the fact that 1 and $h_{11}(\boldsymbol{x})$ are even functions of $\boldsymbol{x}$, so that their product with $\partial_\parallel V(\boldsymbol{x})$, which is an odd function of $\boldsymbol{x}$, has a vanishing integral.

Introducing this result in Eq. (26), we get

$$\kappa_{\text{eff}} = 1 - \frac{\bar{\rho}_2}{F}\int h_{12}(\boldsymbol{x})\partial_\parallel V(\boldsymbol{x})\mathrm{d}\boldsymbol{x}. \tag{30}$$

Finally, using $\bar{\rho}_2 = (1-\tau)\bar{\rho}$ and the definition of K, Eq. (2), leads to Eq. (5):

$$K = \frac{\bar{\rho}}{F}\int \partial_\parallel V(\boldsymbol{x})h_{12}(\boldsymbol{x})\mathrm{d}\boldsymbol{x}. \tag{31}$$

III. COMPUTATION OF THE CORRELATION FUNCTIONS

Our goal is to solve

$$\tilde{A}\tilde{C} + \tilde{C}\tilde{A}^* = 2T\mathbb{1} \tag{32}$$

We denote

$$\tilde{A} = T\begin{pmatrix}\alpha+\mathrm{i}\delta & \beta\\ \beta & \gamma\end{pmatrix}, \tag{33}$$

$$\tilde{C} = \begin{pmatrix}c_{11} & c_{12}\\ c_{21} & c_{22}\end{pmatrix}, \tag{34}$$

where

$$\alpha = 1+\tau_1\tilde{v}, \tag{35}$$

$$\beta = (\tau_1\tau_2)^{1/2}\tilde{v}, \tag{36}$$

$$\gamma = 1+\tau_2\tilde{v} \tag{37}$$

$$\delta = \frac{fk_\parallel}{k^2}, \tag{38}$$

and c_{11}, c_{12}, c_{21} and c_{22} are the unknowns.

Our system of 4 equations with four unknowns (32) writes:

$$\begin{cases}(\alpha+\mathrm{i}\delta)c_{11}+\beta c_{21}+c_{11}(\alpha-\mathrm{i}\delta)+c_{12}\beta &= 2\\ (\alpha+\mathrm{i}\delta)c_{12}+\beta c_{22}+c_{11}\beta+c_{12}\gamma &= 0\\ \beta c_{11}+\gamma c_{21}+c_{21}(\alpha-\mathrm{i}\delta)+c_{22}\beta &= 0\\ \beta c_{12}+\gamma c_{22}+c_{21}\beta+c_{22}\gamma &= 2\end{cases} \Leftrightarrow \begin{cases}2\alpha c_{11}+\beta(c_{12}+c_{21}) &= 2\\ \beta(c_{11}+c_{22})+(\alpha+\gamma+\mathrm{i}\delta)c_{12} &= 0\\ \beta(c_{11}+c_{22})+(\alpha+\gamma-\mathrm{i}\delta)c_{21} &= 0\\ 2\gamma c_{22}+\beta(c_{12}+c_{21}) &= 2\end{cases}$$

$$\Leftrightarrow \begin{cases}\alpha c_{11} = \gamma c_{22}\\ (\alpha+\gamma+\mathrm{i}\delta)c_{12} = (\alpha+\gamma-\mathrm{i}\delta)c_{21}\\ \beta(\frac{\gamma}{\alpha}+1)c_{22}+(\alpha+\gamma-\mathrm{i}\delta)c_{21} = 0\\ 2\gamma c_{22}+\beta(\frac{\alpha+\gamma-\mathrm{i}\delta}{\alpha+\gamma+\mathrm{i}\delta}+1)c_{21} = 2\end{cases} \Leftrightarrow \begin{cases}c_{11} = \frac{\gamma}{\alpha}c_{22}\\ c_{12} = \frac{\alpha+\gamma-\mathrm{i}\delta}{\alpha+\gamma+\mathrm{i}\delta}c_{21}\\ c_{21} = -\frac{1}{\alpha+\gamma-\mathrm{i}\delta}\frac{\beta(\alpha+\gamma)}{\alpha}c_{22}\\ \left[2\gamma - \frac{\beta}{\alpha+\gamma-\mathrm{i}\delta}(\frac{\alpha+\gamma-\mathrm{i}\delta}{\alpha+\gamma+\mathrm{i}\delta}+1)\beta(\frac{\gamma}{\alpha}+1)\right]c_{22} = 2\end{cases} \tag{39}$$

We can solve for c_{22}:

$$c_{22} = \frac{\alpha\left[(\alpha+\gamma)^2+\delta^2\right]}{\alpha\gamma\left[(\alpha+\gamma)^2+\delta^2\right]-\beta^2(\alpha+\gamma)^2}. \tag{40}$$

And the rest follows,

$$\tilde{C}_\Phi = \frac{1}{(\alpha+\gamma)^2(\alpha\gamma-\beta^2)+\alpha\gamma\delta^2} \begin{pmatrix} \gamma\left[(\alpha+\gamma)^2+\delta^2\right] & -\beta(\alpha+\gamma)(\alpha+\gamma-\mathrm{i}\delta) \\ -\beta(\alpha+\gamma)(\alpha+\gamma+\mathrm{i}\delta) & \alpha\left[(\alpha+\gamma)^2+\delta^2\right] \end{pmatrix} \tag{41}$$

Finally, from the values of α, β, γ and δ (35):

$$\tilde{C} = \left[(1+\tilde{v})(2+\tilde{v})^2 + (1+\tilde{v}+\tau_1\tau_2\tilde{v}^2)\frac{f^2k_\parallel^2}{k^4}\right]^{-1} \begin{pmatrix} (1+\tau_2\tilde{v})\left[(2+\tilde{v})^2+\frac{f^2k_\parallel^2}{k^4}\right] & -\sqrt{\tau_1\tau_2}\tilde{v}(2+\tilde{v})(2+\tilde{v}-\mathrm{i}\frac{fk_\parallel}{k^2}) \\ -\sqrt{\tau_1\tau_2}\tilde{v}(2+\tilde{v})(2+\tilde{v}+\mathrm{i}\frac{fk_\parallel}{k^2}) & (1+\tau_1\tilde{v})\left[(2+\tilde{v})^2+\frac{f^2k_\parallel^2}{k^4}\right] \end{pmatrix} \tag{42}$$

IV. LONG-RANGE BEHAVIOR OF THE CORRELATION FUNCTIONS

In order to determine the long-range behavior, we have to compute the inverse Fourier transform of

$$\tilde{C}_0(\boldsymbol{k}) = \lim_{a\to 0}\tilde{C}(ak_\parallel, a^{1/2}\boldsymbol{k}_\perp) = \left[(1+v_0)(2+v_0)^2 + (1+v_0+\tau_1\tau_2v_0^2)\frac{f^2k_\parallel^2}{k_\perp^4}\right]^{-1} \begin{pmatrix} (1+\tau_2v_0)\left[(2+v_0)^2+\frac{f^2k_\parallel^2}{k_\perp^4}\right] & -\sqrt{\tau_1\tau_2}v_0(2+v_0)(2+v_0-\mathrm{i}\frac{fk_\parallel}{k_\perp^2}) \\ -\sqrt{\tau_1\tau_2}v_0(2+v_0)(2+v_0+\mathrm{i}\frac{fk_\parallel}{k_\perp^2}) & (1+\tau_1v_0)\left[(2+v_0)^2+\frac{f^2k_\parallel^2}{k_\perp^4}\right] \end{pmatrix} \tag{43}$$

We denote $k_\perp = |\boldsymbol{k}_\perp|$, hence $k_\perp^2 = \boldsymbol{k}_\perp^2$. In the remainder of this section, we drop the subscript 0 in $\tilde{C}_0$ for brevity.

We are interested in $\tilde{C}_{21}$ and $\tilde{C}_{11}$ that we write

$$\tilde{C}_{21}(\boldsymbol{k}) = A\frac{k_\perp^2(\alpha k_\perp^2+\mathrm{i}fk_\parallel)}{\alpha^2k_\perp^4+\beta^2f^2k_\parallel^2}, \tag{44}$$

$$\tilde{C}_{11}(\boldsymbol{k}) = B\frac{\alpha^2k_\perp^4+f^2k_\parallel^2}{\alpha^2k_\perp^4+\beta^2f^2k_\parallel^2}, \tag{45}$$

where

$$A = -[\tau(1-\tau)]^{1/2}\frac{v_0(2+v_0)}{1+v_0}, \tag{46}$$

$$B = -\frac{1+(1-\tau)v_0}{1+v_0}, \tag{47}$$

$$\alpha = 2+v_0, \tag{48}$$

$$\beta = \left(1+\frac{\tau(1-\tau)v_0^2}{1+v_0}\right)^{1/2}. \tag{49}$$

First, we compute the inverse Fourier transform along the direction of the force,

$$C(x_\parallel, \boldsymbol{k}_\perp) = \int_{-\infty}^{\infty} \mathrm{e}^{\mathrm{i}x_\parallel k_\parallel}\tilde{C}(k_\parallel, \boldsymbol{k}_\perp)\frac{\mathrm{d}k_\parallel}{2\pi}. \tag{50}$$

We compute this integral using the residue theorem, leading to

$$C_{21}(x_\parallel, \boldsymbol{k}_\perp) = \frac{A}{2\beta f}\left[(1+\beta^{-1})\theta(-x_\parallel)+(1-\beta^{-1})\theta(x_\parallel)\right] \times k_\perp^2\mathrm{e}^{-\frac{\alpha|x_\parallel|}{\beta f}k_\perp^2}, \tag{51}$$

$$C_{11}(x_\parallel, \boldsymbol{k}_\perp) = \frac{B\alpha(1-\beta^{-2})}{2\beta f}k_\perp^2\mathrm{e}^{-\frac{\alpha|x_\parallel|}{\beta f}k_\perp^2} + \frac{B}{\beta^2}\delta(x_\parallel). \tag{52}$$

The Dirac term in the tracer-tracer correlation function is the contribution of a tracer with itself. It has no effect on the long-distance behavior. The inverse Fourier transform in the transverse direction is straightforward to compute: we recognize the second derivative of a Gaussian. We get Eqs. (13–17).

V. TRACER-NON TRACER CORRELATION IN FRONT OF THE TRACER AT VANISHING TRACER FRACTION

We focus on the behavior of the tracer-non tracer correlation $C_{21}(\boldsymbol{x})$ for $x_\parallel > 0$, in the limit of vanishing tracer fraction, $\tau \to 0$. Since we are interested in distances large compared to the range of the potential, we may approximate it by a Dirac: $v(\boldsymbol{x}) \to v_0\delta(\boldsymbol{x})$, where $v_0 = \tilde{v}(0) = \int v(\boldsymbol{x})\mathrm{d}\boldsymbol{x}$. Thus, we want to inverse Fourier transform

$$\tilde{C}_{21}(\boldsymbol{k}) = A\frac{k^2}{\alpha k^2 - \mathrm{i}fk_\parallel}, \tag{53}$$

where A and α are given by Eqs. (46) and (48). Using $k^2 = k_\parallel^2 + k_\perp^2$, we can compute the inverse Fourier transform along $k_\parallel$ with the residue theorem, leading to:

$$C_{21}(x_\parallel, \boldsymbol{k}_\perp) = -\frac{A}{2\alpha q}\left(q + \frac{f}{2\alpha}\right)^2 \mathrm{e}^{-x_\parallel\left(q+\frac{f}{2\alpha}\right)}, \tag{54}$$

where we have introduced $q = \left(k_\perp^2 + \frac{f^2}{4\alpha^2}\right)^{1/2}$. Since we are interested in the behavior at large $x_\parallel$, we can use the saddle-point method to compute the inverse Fourier transform in the transverse direction, leading to

$$C_{21}(\boldsymbol{x}) \underset{x_\parallel\to\infty}{\sim} -\frac{Af^{\frac{d+1}{2}}}{(2\pi)^{\frac{d-1}{2}}\alpha^{\frac{d+3}{2}}x_\parallel^{\frac{d-1}{2}}}\mathrm{e}^{-\frac{fx_\parallel}{\alpha}-\frac{fx_\perp^2}{4\alpha x_\parallel}}. \tag{55}$$

The first term in the exponential shows that the decay is exponential. We remark that A is negative, hence the correlation is positive: there is a finite size "traffic jam" in front of the tracers. We also note that the factor $[\tau(1-\tau)]^{1/2}$ in A, which goes to zero when $\tau \to 0$, is removed if we consider the pair correlation function $h_{21}(\boldsymbol{x})$.